EBioMedicine 52 (2020) 102656

Contents lists available at ScienceDirect

EBioMedicine

journal homepage: www.elsevier.com/locate/ebiom

Research paper

Intracavernous injection of size-specific stem cell spheroids for neurogenic erectile dysfunction: Efficacy and risk versus single cells

Yongde Xu[a], Yong Yang[b], Han Zheng[b], Chao Huang[c], Xiaoming Zhu[c], Yichen Zhu[a], Ruili Guan[d], Zhongcheng Xin[d], Zhiqiang Liu[c,*], Ye Tian[a,*]

[a] Department of Urology, Beijing Friendship Hospital, Capital Medical University, No. 95th Yongan Road, Beijing 100050, China
[b] Department of Urology, Fourth Medical Center, Chinese PLA General Hospital, Beijing 100048, China
[c] Institute of military cognitive and brain sciences, Academy of Military Medical sciences, 27 Taiping Road, Haidian district, Beijing 100850, China
[d] Andrology Center, Peking University First Hospital, Peking University, Beijing 100034, China

ARTICLE INFO

Article History:
Received 4 September 2019
Revised 21 January 2020
Accepted 22 January 2020
Available online xxx

Keywords:
Erectile dysfunction
Stem cells
Three-dimensional culture
Pulmonary embolism
Intracavernous injection

ABSTRACT

Background: Intracavernous injection (ICI) of adipose-derived stem cells (ADSCs) has been demonstrated promising for neurogenic erectile dysfunction (ED). However, due to the sponge-like structure of corpus cavernosum (CC) with abundant vessels, ICI was indeed like intravenous injection. Thus, the cell escaping may be a concern of safety and limited therapy, but the issue has not been clearly demonstrated yet.
Methods: Suspensions of free ADSCs (FAs) and ADSCs-based spheroids (ASs) with suitable size were intracavernously injected at doses of 0.5, 1, 2, or 4 million cells. The cell loss and safety after ICI, erectile function and histopathologic change, etc. were analyzed with multimodality of methods.
Findings: Most FAs escaped from sponge-like CC after ICI due to their small size, weakening stem-cell therapeutic efficacy. Worse still, the escaped cells were shown to cause widespread pulmonary embolism (PE), and even death in some animals. Further, it was founded that the therapeutic effect of FAs may be ascribed to the larger cell clusters which spontaneously aggregated before ICI and were trapped within CC after ICI. In comparison, cell loss and PE were significantly avoided by transplanting ASs. Importantly, better therapeutic outcomes were detected after ICI of ASs when compared to FAs with the same cell number.
Interpretation: Transplantation of size-specific ASs instead of single-cell suspension of FAs for neurogenic ED may be a wiser choice to achieve steady therapeutic outcome and to reduce risks for the future clinical application.
Fund: This work was supported by the National Natural Science Foundation of China (81701432) (to Y. Xu). Youth Training Project for Medical science (16QNP129) and Beijing Nova Program of science and technology (Z171100001117115) (to Z. Liu).

1. Introduction

Cavernous nerves (CN) injury-related erectile dysfunction (ED) was common in clinic, especially for those who have received radical prostatectomy (RP) [1–3], the most common treatment for localized prostate cancer. Oral phosphodiesterase type 5 (PDE 5) inhibitors are currently the first-line choice for ED and more than 70% of total ED patient population can be satisfactorily treated by the drugs. However, PDE5 inhibitors are not so effective for neurogenic ED that only ~43% of such patients respond to the drugs [4,5]. At present, no effective treatment was clinically available yet for most of neurogenic ED patients.

In recent years, numerous preclinical and clinical studies have demonstrated that stem-cell (SC) therapy was of great potential for patients with neurogenic ED [6–8]. Autologous, allogeneic or even xenogenic adipose-derived stem cells (ADSCs) have become the most widely used SC type for ED primarily because of their abundant distribution in adult and low immunogenicity [9]. Among those studies, intracavernous injection (ICI) was the most frequently adopted route for SC transplantation [10]. Despite the encouraging achievement in total in the field, it could not be ignored that the therapeutic outcomes varied with studies for which the reasons were unknown. Bahk et al. found that erectile function partially restored after ICI of SCs; however, the hardness of the penile erection remained insufficient for penetration [11]. In this study, the researchers have tried to clamp the root of penis for 30 min to improve therapeutic effect by increasing cell retention in corpus cavernosum (CC). In another study, Yiou et al. found that the partially recovered erectile function

* Corresponding authors.
E-mail addresses: zhiqiangliu_amms@163.com (Z. Liu), tianye_uro@163.com (Y. Tian).

https://doi.org/10.1016/j.ebiom.2020.102656

Research in context

Evidence before this study

In our previous study, scaffold-free ADSCs spheroids were firstly transplanted via intracavernous injection for erectile dysfunction (ED) instead of single-cell suspension of ADSCs (free ADSCs, FAs) and therapeutic outcomes were much improved. We supposed the main cause may be that the large size of spheroids prevented cell loss against sponge-like structure of corpus cavernosum (CC), which, however, has not been fully proved. In addition, deaths associated with stem cell injections were not uncommon in clinical practice. Several studies have reported that fatal pulmonary embolism events may occur upon intravenous injection (IVI) of stem cells (SCs).

Added value of this study

The study was the first report about the potential risk of stem cell transplantation for neurogenic ED via ICI, and the underlying cause why therapeutic outcomes by ICI of stem cells have been inconsistent in different studies. The novel findings of the study included: (1) ICI was essentially like IVI because of the sponge-like structure with abundant vessels in CC and thus, it was a high risk approach for stem cell transplantation which may lead to PE, or even death; (2) Formation of scaffold-free spheroids, whose sizes could be controlled by adjusting cell numbers, was an efficient method to trap stem cells in CC, improving therapeutic efficacy and avoiding PE. (3) Therapeutic benefits by ICI of free stem cells were mainly due to cell self-aggregation before injection which may result in large aggregates easily trapped in CC. This may be also the cause why therapeutic outcomes varied with studies.

Implications of all the available evidence

Our study demonstrates that ICI of free stem cells is of low efficacy, high risk and should be cautiously adopted in practice. These data, together, implicate that ICI of stem-cell spheroids instead of free cells appears to be a sounder option for future clinical application.

declined again over time after ICI of SCs [6]. The above studies suggest that a single ICI of SCs was likely insufficient, and repeated injections or other strategies may be required.

In addition, intravenous injection (IVI) of stem cells has been definitely reported by independent groups that it could lead to the potentially lethal condition with the escaped cells being rapidly trapped in lung [12–14]. Meanwhile, some clinical studies have also found serious complications such as pulmonary embolism (PE) and even death among patients after IVI of stem cells [15,16]. As is known, the CC is a sponge-like structure with abundant vessels [17] and thus it is essentially an intravenous approach too. Thus, we hypothesized that free SCs loss with blood flow after ICI may be the main cause of inefficient therapeutic outcomes as mentioned above. In addition, acute PE ascribed to SCs after ICI may be a safety concern, like that after IVI of SCs. To date, no safe cell-dose for treating ED has been identified in the published clinical studies. Therefore, enough attention should be paid to this issue when it comes to the potential risks of patients in future clinical trials.

For these reasons, an approach to retaining cells in CC can look forward to improving therapeutic efficacy and avoid potential risks when treating ED with SCs. Herein, a systemic study was designed to explore the evidence for the above hypothesis. On the basis, transplanting size-specific stem cell spheroids to improve therapeutic efficacy and reduce risks after ICI for neurogenic ED was proposed and investigated.

2. Materials and methods

2.1. Experimental design

16-week-old male Sprague-Dawley (SD) rats were used in this study. All animal procedures and their care were conducted in conformity with animal ARRIVE guidelines and was approved by Institutional Animal Care and Use Committee of the General Hospital of the People's Liberation Army (Beijing, China). All animals were maintained under controlled temperature (23±2 °C) and light (12-h light/dark cycle) conditions with standard diet and water.

The rats were anesthetized with 3% pentobarbital sodium, the prostate glands were exposed via a ventral midline incision, and the posterolateral CNs and major pelvic ganglia (MPG) were easily identified. Twelve SD rats were randomly assigned to the sham group (i.e., exposing and isolating CNs, without crushing CNs) and received an ICI of 0.2 ml phosphate buffer solution (PBS). In the other 120 rats, the CNs were isolated and crushed bilaterally using a microsurgical needle holder [18]. On the same day of surgery, the rats that underwent bilateral CNs injury were randomly divided into three groups: those who received an ICI of 0.2 ml PBS (n = 24 animals), free ADSCs suspension (abbreviated to FAs, 0.5×10^6, 1×10^6, 2×10^6 and 4×10^6 cells in 0.2 ml PBS, n = 12 animals per dose), or ADSCs-based spheroids (abbreviated to ASs, 500, 1000, 2000 and 4000 ASs in 0.2 ml PBS, 1×10^3 ADSCs per spheroid, n = 12 animals per group). 24 h after ICI of 0.2 ml PBS, erectile function test was conducted in 12 model rats. The remaining 108 animals were sacrificed, and their penises were harvested for subsequent analysis after erectile function test at day 28.

We investigated the retention of injected ASs and FAs using *in vivo* bioluminescence imaging. ADSCs co-expressing firefly luciferase (Luc) and green fluorescent protein (GFP) were specifically used for this part. Twelve normal SD rats were randomly divided into two equal groups: those receiving an ICI of Luc^+-GFP^+ FAs (1×10^6 cells in 0.2 ml PBS) and those receiving Luc^+-GFP^+ ASs (1000 ASs in 0.2 ml PBS).

To assess PE, designated rats that underwent bilateral CNs injury were randomly divided into three groups: those receiving an ICI of 0.2 ml PBS (n = 6 animals), FAs (0.5×10^6, 1×10^6, 2×10^6 and 4×10^6 cells in 0.2 ml PBS, n = 6 animals per dose), or ASs (500, 1000, 2000 and 4000 ASs in 0.2 ml PBS, 1×10^3 ADSCs per spheroid, n = 6 animals per group). All rats were sacrificed after ICI, the lungs were harvested and stained by hematoxylin and eosin (HE). The degree of PE in each group was quantified by a self-defined scoring system. Score 0 implied that no PE was observed under microscope (HE staining, 40 ×). Score 1 was recorded for thrombus formation in less than 2 sites, score 2 was recorded for thrombosis in 3 sites, and score 4 was recorded for thrombus formation in no less than 4 sites. Theoretically, PBS injection should not cause any PE, but from H&E stained sections, some suspected PE may exist and score more than 0. To use PBS injection group as no-PE control, the highest PE score in PBS group was set as the threshold of background.

2.2. ASs generation, and ADSCs self-aggregation

Human ADSCs were isolated from human adipose tissue abandoned after liposuction, which was approved by the ethical committee of the General Hospital of the People's Liberation Army (Beijing, China). Relevant informed consent forms were signed by each donor before specimen collection. ADSCs were cultured in low-glucose Dulbecco's Modified Eagle Medium (DMEM; HyClone, Logan, UT, USA). ADSCs (3~5 passages) and used to generate ASs using the hanging drop method as previously described [19]. Briefly, the cultured ADSCs were harvested via trypsinization and re-suspended in DMEM supplemented with 5%

fetal bovine serum (FBS; HyClone). Free cell suspensions were prepared at concentrations of 2×10^4 cells/mL, 4×10^4 cells/mL, 8×10^4 cells/mL, 1.6×10^5 cells/mL, and 3.2×10^5 cells/mL, respectively. Hanging drops were prepared at 37 °C in a humidified atmosphere of 5% CO_2 using the free-cell suspension described above. Designated hanging drop of 25 μL was observed continuously for 5 days to dynamically assess the pattern of ASs formation. On Day 3 of the culture, ASs containing 1000 cells were collected to treat neurogenic ED.

The re-suspended ADSCs were adjusted to different concentrations: 2.5×10^6 cells/mL, 5×10^6 cells/mL, 1×10^7 cells/mL, and 2×10^7 cells/mL. The above free-cell suspensions were placed *in vitro* for 5 min, 10 min, 30 min, 60 min, and 90 min, and the self-aggregation of ADSCs was observed dynamically.

2.3. Measurement of the traversability of CC and pulmonary circulation via polystyrene microspheres

The polystyrene microspheres (PSMs, Tianjin BaseLine ChromTech Research centre, Tianjin, China) used in this study had different particle sizes (diameter of particles = 7.962 μm to 158.866 μm). The consistency was 0.378, D50 = 60.941 μm, D10 = 26.781 μm, D90 = 102.844 μm, and D (4, 3) = 63.441 μm. Blood samples were respectively collected from postcava and ventral aorta immediately as well as 5, 10, and 15 min after ICI of PSMs. Blood smears were observed under a microscope to measure the maximum diameter of PSMs intercepted at the different time points. These data were used to estimate the size of the particles that could be trapped by the CC and pulmonary circulation.

2.4. Measurement of intracavernous pressure and mean arterial pressure

Four weeks after CNs crush injury or sham operation, the intracavernous pressure (ICP) and mean arterial pressure (MAP) were measured respectively, as previously described [20,21]. Briefly, anesthesia of rats with 3% pentobarbital sodium, the bilateral CNs were exposed via a ventral midline incision. A 25-gage butterfly needle connected to a PE-50 tube filled with heparinized saline (200 IU/mL) was inserted into left CC. The other end of the PE-50 tube was connected to a data acquisition system (MP150; Biopac Systems Inc, Goleta, CA, USA). The CN was isolated and hooked by a bipolar stimulation electrode (each pole was 0.2 mm in diameter, separated by 1 mm) 3 ~ 4 mm distal to the MPG. The stimulus parameters were 20 Hz, pulse width of 0.2 ms, 1.5 mA, and duration of 60 s via a signal generator (Biopac Systems Inc, Goleta, CA, USA). Three electrostimulations were conducted on either CN separately, and the maximal amplitude of ICP was calculated from baseline value. MAP was recorded using a 25- gage butterfly needle inserted into the aorta at the level of the iliac bifurcation. The ratio of maximal ICP (mmHg) to mean MAP (mmHg) was calculated to normalize for variations in systemic blood pressure.

2.5. Fluorescence microscopy and histological staining

Freshly dissected penis (mid-shaft portion) and lungs were fixed with 2% formaldehyde and 0.002% picric acid in 0.1 M phosphate buffer for 4 h, followed by overnight immersion in 30% sucrose. Tissues were frozen in optimum cutting temperature compound (Sakura Finetek, Torrance, CA, USA) and stored at - 80 °C until use. Sections were cut at 5 micrometers and subjected to next tests.

Smooth muscle in penis was stained with AlexaFluor-488 conjugated phalloidin (Life Technology, A12379) or rabbit anti-alpha smooth muscle actin (α-SMA; 1:1000; Abcam, ab124964). Rabbit anti-neuronal nitric oxidesynthase (nNOS, 1:400; Abcam, ab76067) was used to evaluate the number of nNOS-positive nerves in CC. Vascular endothelium in lung and in CC was stained with mouse anti-CD 31 (1:500; Abcam, ab24590). Semiquantitative data of the nerves involved in penile erection by calculating the ratio of the number of nNOS-positive fibers to phalloidin-positive area. Cell nucleus were stained with 40,6-diamidino-2-phenylindole (DAPI; Invitrogen, Carlsbad, CA, USA).

Because of the expression of GFP, the retaining ADSCs in the dissected lungs could be observed directly using an inverted fluorescence microscope. The lungs of rats who died suddenly during or immediately after ICI were stained with hematoxylin–eosin staining. Slides were photographed and recorded using a LEICA DFC 425 C digital microscope camera system (Leica). Computerized histomorphometric analysis was performed using the Image-Pro Plus 6.0 software (Media Cybernetics).

2.6. Lentivirus transfection and in vivo bioluminescence imaging

Lentivirus vector pCDF-MSCV-Flu-EF1-GFP-T2A-Puro was constructed. Then, packing plasmids pMD2.G and psPAX2 were employed for co-transfecting 293T cells with lentivirus vectors at the ration of 1:2:3. A total of 1.5ug plasmids were used for one well of 6-well plate. Lentiviral particles were collected at 48 h and 72 h after trensfection. Ultrafiltration Tube was used for lentivirus concentration. Lentivirus were added into ADSCs at MOI of 10~20 and incubated for 24 h. The successfully infected cells were screened by puromycin.

Bioluminescence imaging was performed using a Xenogen IVIS 100 imaging system. Rats were anesthetized by 3% pentobarbital sodium. 50 mg/kg D-luciferin (Thermo) was intracavernously injected before imaging and cell suspensions were supplemented with 300 μg/mL D-luciferin. Imaging was performed immediately as well as at 10 min, 60 min and 3 days after ICI. Signals were acquired for 1 min until peak signal was observed. Fluorescence signal from a fixed region of interest was estimated using the Living Image 4.0 software (Xenogen).

2.7. Western blot analysis

The cellular protein samples were prepared by homogenization of penile tissue in a lysis buffer containing 1% IGEPAL CA-630, 0.5% sodium deoxycholate, 0.1% sodium docecyl sulfate, aprotinin (10 mg/mL), leupeptin (10 mg/mL), and phosphate buffered saline. The cellular lysates from penis containing 20 mg of protein were electrophoresed in sodium dodecyl sulfate–polyacrylamide gel electrophoresis and then transferred to a polyvinylidene fluoride membrane (Millipore Corp.). Primary antibodies were rabbit anti-α-SMA (1:1000; Abcam), rabbit anti- nNOS (1:400; Abcam) and rabbit anti-GAPDH (1:2000; cwBio, Lot:01225/50,404). After the hybridization of secondary antibodies, the resulting images were analyzed with ChemiImager 4000 (Alpha Innotech Corporation, San Leandro, CA, USA).

2.8. Statistical analysis

Partial data were expressed as mean ± standard deviation and other data were expressed as mean and Upper/Lower limits. One-way analysis of variance (ANOVA) followed by Tukey`s post hoc test was used to identify statistically significant differences among groups; A two-group comparison was done using *t*-test. All data analyses were performed using SPSS statistical software (version 17.0; SPSS Inc.). Values of $p < 0.05$ were considered statistically significant.

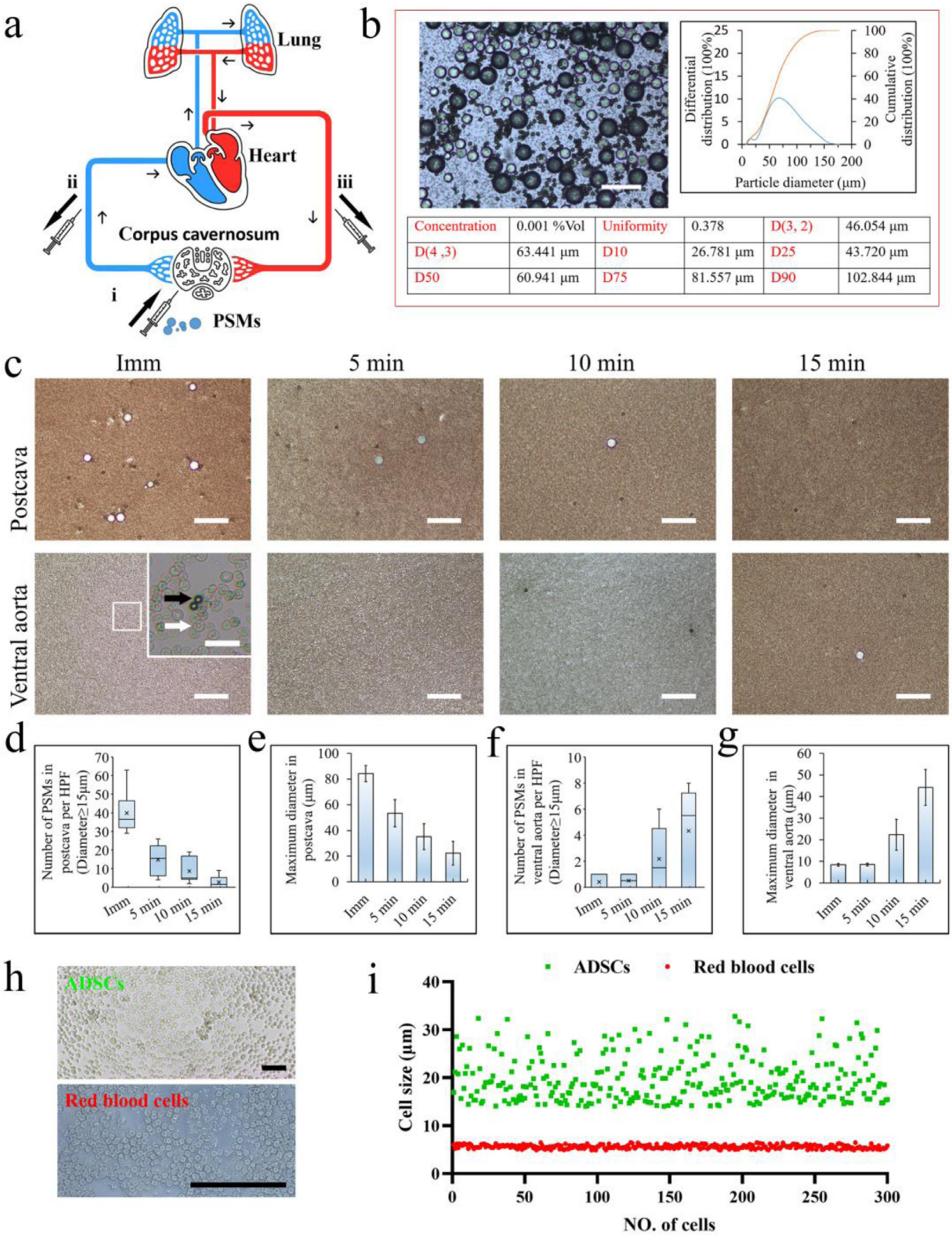

Fig. 1. Measurement of the traversability of the CC and pulmonary circulation using monodisperse polystyrene microspheres (PSMs). (a) Scheme illustrating the measurement of the traversability of the CC and pulmonary circulation. (i) ICI of PSMs with different particle sizes. (ii) Blood from postcava was collected immediately as well as 5, 10, and 15 min after ICI. (iii) Abdominal aortic blood was collected immediately as well as 5, 10, and 15 min after ICI. Arrows indicate the direction of blood flow. (b) Size distribution of PSMs before injection. Scale bar = 200 μm. (c) PSMs detection on blood smears at different time points. Scale bar = 200 μm. Inset: magnified image. White arrows indicate red blood cells (RBCs). Black arrows indicate PSMs. Scale bar = 20 μm. (d) and (e) The number of PSMs larger than 15 μm in diameter detected on postcava blood smear after ICI (per 100 × field) and the maximum diameter of PSMs. (f) and (g) Equal detection of PSMs in ventral aorta blood by smear. The data are based on blood cell smears from six animals per group. (h) and (i) The size of human ADSCs and rat RBCs. The diameter of ADSCs and RBCs was 19.72 ± 6.47 μm and 5.61 ± 0.40 μm, respectively. Scale bar = 100 μm. (For interpretation of the references to color in this figure legend, the reader is referred to the web version of this article.)

3. Results

3.1. Estimating the pore size in the CC and pulmonary circulation by PSMs

Blood samples from postcava and ventral aorta were collected immediately as well as at 5, 10, and 15 min after ICI of PSMs (Fig. 1a–c). The numbers of PSMs were expressed as mean and Upper/Lower limits and the maximum mean diameters observed at different time points were expressed as mean ± standard deviation (Fig. 1d–g). The number of microspheres larger than 15 μm were rarely detected in the blood from ventral aorta, suggesting lots of PSMs may have been trapped in pulmonary circulation, When the abdominal aortic blood was collected immediately after ICI of PSMs, those with a diameter similar to erythrocytes (approximately 5.61 ± 0.40 μm, Fig. 1h and i) were observed. The results indicated that the maximum pores allowing cell loss were about 80~100 μm in CC, easy for single-cell ADSCs loss (cell size was 19.72 ± 6.47 μm, Fig. 1h and i); while most of the ADSCs escaping from CC would be captured in the pulmonary circulation.

3.2. Size-controlled formation of cell spheroids under gravity-enforced 3-dimensional culture

After 3 days of culture, most of cells in hanging drops formed morphologically stable spheroids and thereafter, the appearance of the spheroids changed little (Fig. S1a and b). The cell number was the sole factor influencing the sizes of spheroids and they were positively correlated with the cell numbers ((Fig. S1c). At day 3, the diameters of the spheroids formed by 500, 1000, 2000, 4000, and 8000 cells were 107.56 ± 25.68 μm, 153.26 ± 23.74 μm, 173.20 ± 23.30 μm, 232.30 ± 19.62 μm, and 304.47 ± 19.73 μm, respectively. The results indicated that the sizes of spheroids could be controlled by adjusting stem cells numbers.

3.3. Safety assessment

After ICI of a low dose (0.5×10^6) ADSCs, no rat death was observed. However, deaths increased with injected cell doses that 1/12 (8.3%, cell dose = 1×10^6), 2/12 (16.6%, cell dose = 2×10^6) and 3/12 (25%, cell dose = 4×10^6) deaths happened within 24 h (Fig. 2a). In comparison, no death happened after cell spheroid injection even at high dose.

The PE scores in rats receiving free-cell suspension were increased with cell doses and significantly higher than those receiving PBS injection at each dose ($P<0.05$, Fig. 2b, Tables S1 and S2). No statistical significance was detected between ASs injection and PBS injection at each dose (Table S2). As expected, significant PE appeared in lungs of died rats, which was not detected in PBS-injected rats (Fig. 2c). Surprisingly, PE was detected in all FAs injected rats, while no significant PE was observed in spheroids injected ones.

To provide direct evidence that PE was resulted from injected ADSCs, a longitudinally sectioned pulmonary microvessel was identified under high-magnification microscope (Fig. 2d). As can be seen from the image, some nucleated cells which may be ADSCs accumulated in the pulmonary microcirculation, resulting in the accumulation of red blood cells in the rear and the formation of embolism. More importantly, Dil-labeled cells were found in the pulmonary vessels (Fig. 2e).

3.4. Erectile function evaluation

At 28 days after ICI, the intracavernous pressure (ICP) and mean arterial pressure (MAP) were determined (Fig. 3a). Compared with normal SD rats (normal group, 0.69 ± 0.03), a sham operation without crushing the CNs (sham group, 0.69 ± 0.02) did not affect erectile function ($P > 0.05$). At 28 days after the bilateral CNs injury (0.29 ± 0.04), even without ADSCs treatment, the ICP_{max}/MAP_{mean} was higher than that measured immediately after injury (0.19 ± 0.03), which suggested that erectile function partially and spontaneously recovered 28 days after CNs injury. At the same cell dose, ICI of ASs improved erectile function better than that of FAs (Fig. 3b and c). Dose-dependent improvement of erectile function was significantly different between ASs and FAs injection. In ASs injection groups, when the total cell number reached 1×10^6, the ICP_{max}/MAP_{mean} value reached the maximum and no further improvement was detected with the increasing cell dose. However, dose-dependent improvement of erectile function in FAs injection groups was detected from the lowest does to the highest does. An explanation for the phenomenon may be that 1×10^6 cells were enough for neurogenic ED when ASs were used as cells could be effectively retained in CC. However, higher doses of FAs must be used to achieve similar efficacy as ease loss of free cells from CC.

3.5. Histomorphometric and western blotting analysis

The nNOS-expressing nerves can relax the smooth muscle of CC through the NO-cGMP signaling pathway and play a key role in maintaining an erection. After ICI, both ASs and FAs improved the nNOS levels compared with control as assessed by immunostaining and western blotting (Fig. 4a and b). It was showed that the number of nNOS-positive nerve fibers per phalloidin-positive area (nNOS/Pha) was significantly lower in rats with CNs injury (CNI) than that in sham (Fig. 4c). At the same cell-dose, the ASs group had a relative higher nNOS level than the FAs group (Fig. 4d). The dose-dependent improvement of nNOS in ASs- and FAs- injected groups were similar to that of erectile function. No significant difference of α-SMA expression was detected between AS- and SA-injected groups (Fig. 4e).

3.6. The fate of stem cells after ICI

As demonstrated in Fig. 5a, stem cell fate after ICI was tracked by bioluminescent (BLI) imaging at several time points. After ICI, the initial BLI signal was significantly higher in the ASs group than that in the FAs group (Fig. 5b and c), suggesting that many free ADSCs had already escaped from CC immediately after ICI. The BLI signal decayed rapidly in FAs-injected group, which was only 31.55% of the starting value at 60 min (Fig. 5d). In comparison, the BLI signal in ASs-injected group was not significantly altered within 60 min. Three days later, a relatively strong BLI signal remained detectable in the ASs-injected group, while only a weak one was detected in the FAs-injected group (Fig. 5b and e).

To determine the fate of the escaped ADSCs, the heart, lungs, liver, and kidneys of animals were harvested for imaging after ICI of ASs or FAs (Fig. 6f and g). The BLI signal was found only in the lungs of the animals receiving FAs injection (Fig. 5g). Histological detection under fluorescent microscope provided further evidence that lots of GFP-positive ADSCs appeared only in lungs of FAs injected animals (Fig. 5k). The results indicated that size-specific ASs were effectively trapped within CC, while numerous FAs escaped from CC and were captured in lung.

3.7. The cause underlying the therapeutic benefit after ICI of free ADSCs

Though the pore size in CC was much larger than the diameters of ADSCs, a small portion of FAs was still successfully trapped within CC after ICI. We supposed it may be due to the self-aggregation of FAs before ICI, because cells must be suspended at high concentration and transported for injection. For verification, suspended FAs were observed under inverted microscopy, which showed that self-aggregation occurred with time and was positively correlated with cell concentrations (Fig. S2).

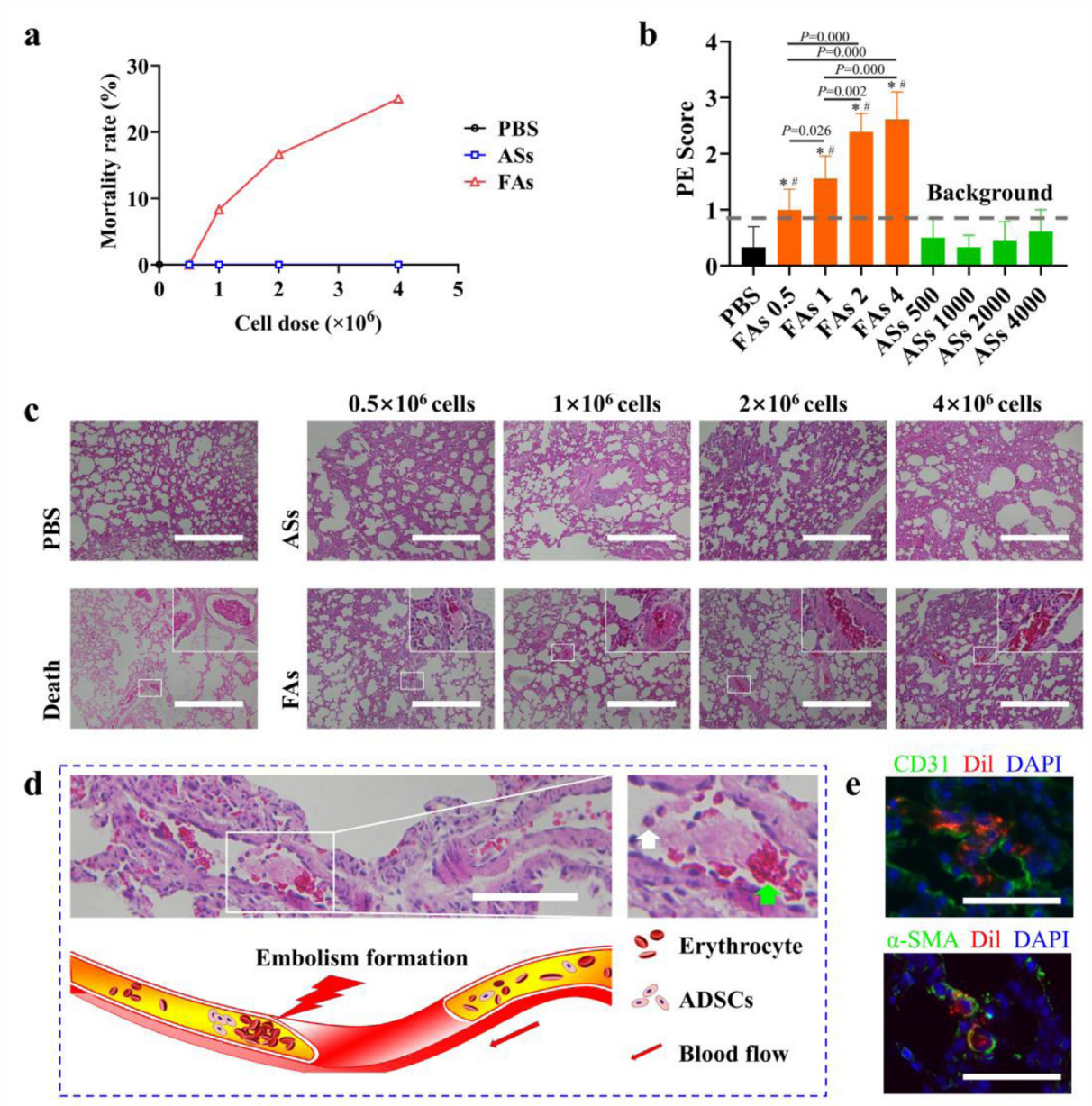

Fig. 2. Safety assessment. (a) Mortality rate within 24 h after ICI. (b) Scoring of PE formation in each group. Score 0 implied that no pulmonary embolism was observed under microscope (HE staining, 40 ×). Score 1 was recorded for thrombus formation in less than 2 sites, score 2 was recorded for thrombosis in 3 sites, and score 3 was recorded for thrombus formation in no less than 4 sites. * denotes $P < 0.05$ vs. data from the PBS group (ANOVA analysis). # denotes $P < 0.05$ vs. data from the same cell-dose ASs group (ANOVA analysis). (c) Pulmonary embolism detection by H&E staining. Scale bar = 500 μm. (d) Typical formation (upper) and schematic illustration (under) of PE in a pulmonary microvessel. The accumulation of ADSCs in the pulmonary microcirculation led to hemodynamic change and eventually led to embolism. White boxed area in the left graph is magnified and shown in the right image. White arrow denotes some nucleated cells in the pulmonary microcirculation. Green arrow denotes a thrombus formed by accumulation of red blood cells. Scale bar = 200 μm. (e) DiI-ADSCs in the pulmonary vessel. CD 31 staining (upper) for vascular endothelium and α-SMA staining (under) for vascular smooth muscle. Scale bar = 100 μm. (For interpretation of the references to color in this figure legend, the reader is referred to the web version of this article.)

We further supposed that self-aggregated FAs trapped in CC may work in the similar way, resulting in therapeutic benefit like trapped ASs. To confirm this, cells were labeled by DiI and placed *in vitro* for 60 min before injection. Penises were sampled at different time points for tracking the *in situ* changes of trapped cells. At 12 h after injection, the cells trapped in CC were primarily in the form of irregular cell clusters, and single cells were rarely seen. Three days after injection, cell clusters began to disperse, and some entered the subendothelial tissues. One week after the injection, ADSCs primarily accumulated near the sinusoidal endothelium or within the subendothelial tissue. Two weeks after the injection, ADSCs were rare and primarily distributed in the subendothelial tissue. The changing patterns were similar between ASs and FAs *in situ* except that more DiI-labeled cells could be observed in the ASs group (Fig. 6a and b).

Two weeks later, immunofluorescence staining was performed to determine the differentiation of engrafted ADSCs in situ. None of the ADSCs retained in the CC was detected to express α-SMA, CD31, or GFAP (see Fig. 6c), suggesting the therapeutic benefits in both groups may not be due to differentiation of the trapped ADSCs.

4. Discussion

Prostate cancer is one of the most common malignancies among men, and radical prostatectomy (RP) is a preferred treatment for patients with early-stage localized prostate cancer. CNs injury-

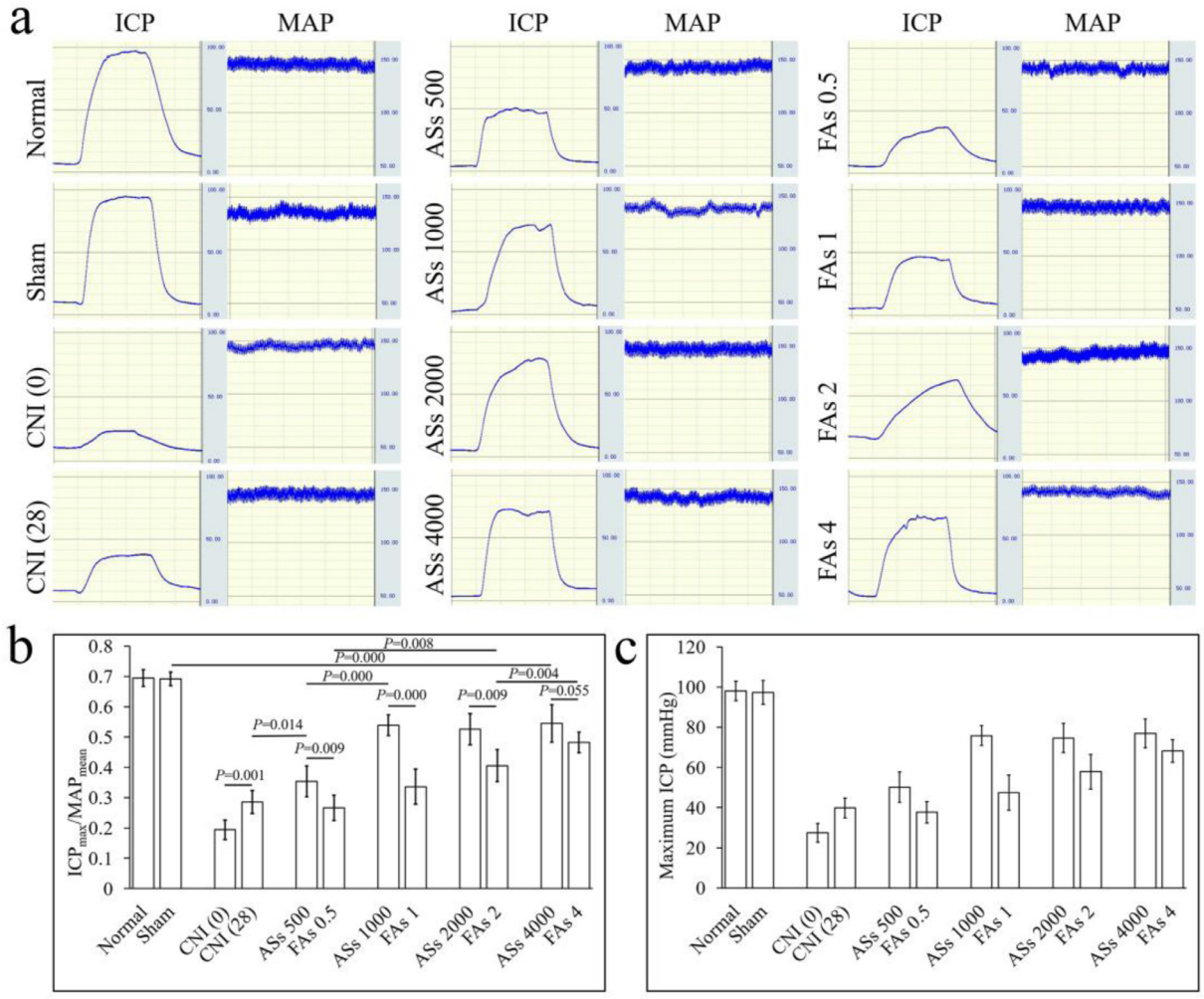

Fig. 3. Evaluation of erectile function. (a) Left: Representative ICP on electrostimulation of the cavernous nerve. Right: Representative pressure of the carotid artery of each group. (b) Ratio of maximum ICP to mean MAP. ANOVA analysis was used to identify statistically significant differences among groups; A two-group comparison was done using *t*-test. (c) Bar graphs represent the maximum ICP detected at 28 days.

related erectile dysfunction (ED) was common in clinic, especially for those who have received RP [1–3,22,23]. Clinically, PDE 5 inhibitors are the most commonly used drugs in patients with post-RP ED; however, their efficacy is far from satisfactory [4,5,24,25]. In recent years, it has been demonstrated by independent studies that ICI of single-cell suspension of ADSCs had a positive therapeutic effect on patients with ED [11,26,27]. For clinical application in future, safety should be firstly considered. However, because of the small number of patients included in previous studies, the extant data are insufficient to prove that SC-for-ED therapy is safe. In addition, there were also lack of thorough investigation about the potential safety issues of SC-for-ED via ICI in animal experiments.

Several studies have reported that fatal PE events might occur upon IVI of SCs [15,16]. Different from most of other tissues, CC is a sponge-like structure where vessels are abundant [17]. Thus, ICI is essentially similar to IVI, for which the present study provided direct evidences using PSMs of varying diameters. Measurement of PSMs from postcava blood and abdominal aortic blood indicated that injected microspheres rapidly escaped from injection site. More importantly, the pore size contrast in CC and lung made it of higher risk for PE formation that vessels in CC allowed larger sizes of cells or cell clusters (smaller than ~84 μm) to pass than pulmonary microcirculation (normally only allowing red blood cells to pass through).

In this study, high incidence of PE was observed in rats receiving free ADSCs injection though in most cases it was non-lethal. These results suggested that ICI of stem cells should also be cautiously treated as IVI. It was noted that high PE risk and animal mortality were related to high cell doses in the present study. Previously, the most commonly used cell dose for ICI was 1×10^6. Below the dose level, only 1/12 animal death was observed in this study. Such low mortality may be more likely to be considered as an accident by investigators but PE risk. It may be why ICI-relayed animal death was rarely reported in previous studies. Meanwhile, it was difficult to detect PE unless dissecting the animals. Therefore, the potential risks (PE or even death) via ICI of stem cells may have been underestimated. To expose the potential risk of ICI, the study set a cell-dose gradient from 0.5×10^6 to 4×10^6 for ICI so as that higher mortality could be achieved and thus attract more attention to the issue. As expected, high animal mortality occurred when dose level exceeded 2×10^6, accompanying with serious PE. The results provided direct evidence for the risk of ICI. Of course, results from animals were not equal to human, the above PE risk may be lower in human because of the larger size of human body that escaped cells from CC could be more diluted. Despite, the results indicated the existence of PE after ICI and should be cautiously treated. Several strategies may be helpful to prevent or reduce PE risk of ICI, including prior vasodilation of the pulmonary blood vessels, cell number calculation, and controlling injection speed. In addition, the study suggested that ICI of size-specific spheroids was safe and provided another way to reduce PE risk for ICI of stem cells.

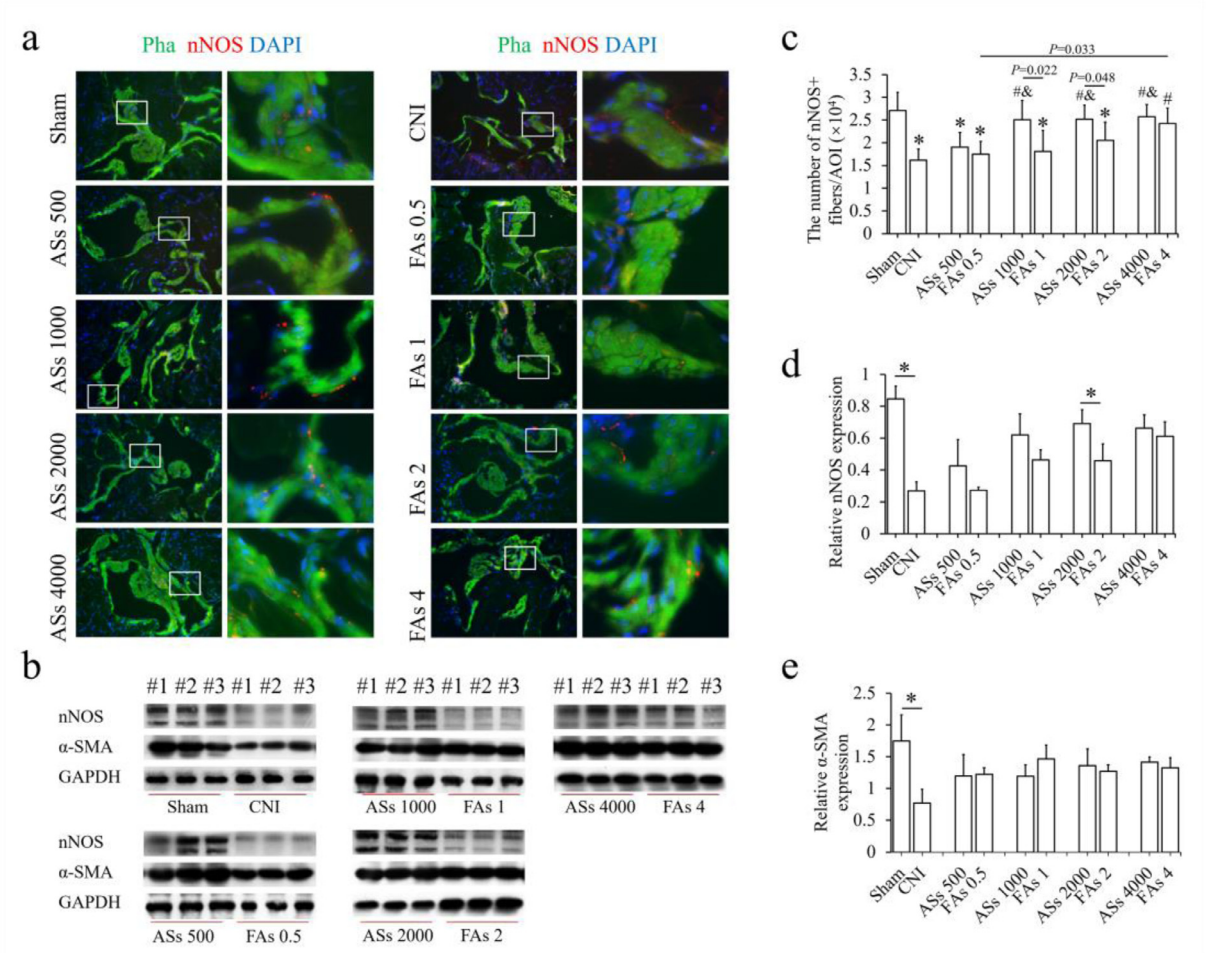

Fig. 4. Assessment of the changes in the nNOS-positive nerves and smooth muscles of the CC. (a) Phalloidin staining for actin and immunostaining for nNOS in a penile midshaft specimen. scale bar = 200 μm. (b) Protein expression of α-SMA and nNOS as evaluated by a Western blot analysis. (c) Semiquantitative quantification of the nNOS-positive fibers per phalloidin-positive area. * denotes $P< 0.05$ vs. the sham group (ANOVA analysis). # denotes $P< 0.05$ vs. the bilateral cavernous nerves injury (BCNI) control group (ANOVA analysis). & denotes $P< 0.05$ vs. the ASs 500 group (ANOVA analysis). (d) Relative nNOS expression to GAPDH by western blotting. * denotes $P< 0.05$ (t-test). (e) Relative α-SMA expression to GAPDH by western blotting. * denotes $P< 0.05$ (t-test). A total of three replicates were tested, with representative images selected from the similar level and position of penile midshaft specimen.

From the data, it is difficult for ADSCs whose diameters are about 19.72 ± 6.47 μm to be retained in the CC. The study confirmed that the retention of stem cells may be due to the self-aggregation before ICI which would result in larger cell clusters. We supposed this may be one of the main causes underlying unsteady efficacies in stem cell-based ED therapy besides other factors as reported previously [6, 11], because the cell dose and aggregation may vary with studies. Therefore, we can logically divide the injected FAs into two parts: (1) the larger cell clusters formed by self-aggregation before ICI which could be trapped in CC after ICI and could play a key role for ED treatment; (2) the smaller cell clusters and free cells which could escape from CC and could be intercepted in the lung (see illustrative schematic in Fig. 7). In this study, we found that the ADSCs intercepted in the lungs existed primarily in the form of single cells, whereas those trapped in CC existed mostly in the form of clusters. These differences provide supporting evidence for the above classification.

Thus, strategies preventing cell escape from CC may be significant for enhancing therapeutic outcomes. In fact, such strategies have been tried by different groups previously. A typical one was magnetic-forced cell retention reported by Lin et al. [28,29]. As expected, the authors demonstrated even a low-dose injection of magnetized ADSCs can result in a therapeutic benefit due to their effective retention in the penis. However, the cytotoxicity of nanoparticles as well as the additional damage caused by the implantation and removal of the magnetic rod are not conducive to future clinical applications. Injectable scaffolds, e.g., microcarriers of relatively large sizes, may be helpful to trap ADSCs within CC. At present, several microcarriers have been reported to deliver cells for therapeutic purpose [30,31], but it should be noted that even those clinical grade materials need to be cautiously evaluated when adopted in novel application.

Previously, some researchers have employed less injection volume and short-term occlusion for ICI, which may be also effective to enhance cell retention in CC under suitable conditions [32,33]. Theoretically, with the same cell number, less volume means higher cell concentration, and higher cell concentration will result in cell aggregation more easily prior injection as we demonstrated in the study. From the point, less ICI volume may improve the cell retention in CC after injection, but more precise syringe and manipulation should be considered to ensure the cell injection, as the smaller the volume, the more difficult the accurate injection. In addition, high volume ICI would also increase the risk of damage to rat penis and thus, less ICI volume needed to be considered too from the view of minimally invasive. In previous studies [8,20,21,28], lots of publications employed 200 μL volume for ICI, the present study also employed the injection volume according to these references. Though no significant damage to CC was observed, it did not mean the injection volume was optimal or even suitable. Actually, there was still lack of an investigation about the optimal volume for ICI in rat models and therefore, the issue deserved in-depth investigation.

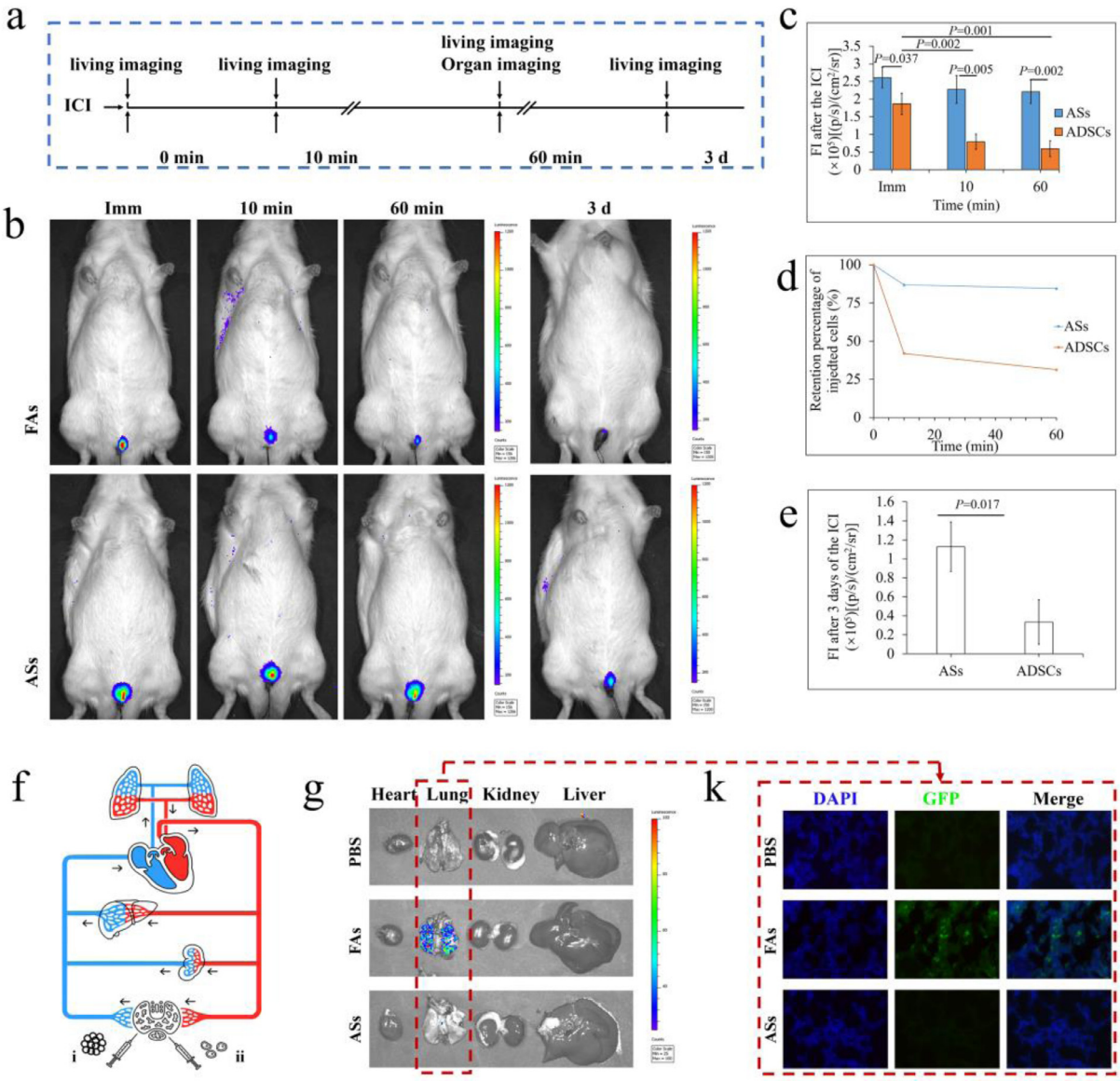

Fig. 5. Tracing the fate of ADSCs after ICI. (a) Schematic representation of the experimental procedure. (b) Representative images of *in vivo* bioluminescent imaging immediately as well as 10 and 60 min and 3 days after ICI. (c) Comparable bioluminescent signal from the two groups. (d) The percentage changing of bioluminescent signal during the first 60 min after injection in the two groups. (e) bioluminescent signal 3 days after injection. (f) Schematic view of the cell fate with blood flow after ICI. i) ICI of ASs. ii) ICI of FAs. Arrows indicate the direction of blood flow. (g) Detection of bioluminescence signal in the heart, lungs, liver, and kidneys after the ICI. (k) Observation of the GFP-ADSCs in the lung tissue using a fluorescent microscope.

Moreover, one should keep in mind that published method is not necessarily the best, many other factors should be considered according to the specific situation when selecting an experimental method. Another issue needs to be pointed out is that the present study used 25 G needle for cell injection, considering that smaller gage may limit sphere size. In fact, 27 or 32 G needle may be more suitable for ICI if only single cell suspension was injected.

In Bahk JY and colleagues' study [11], the penile root of patient was clamped for 30 min to increase the residence time of transplanted cells. It may be effective to retain more cells within CC to some extent, but numerous cells would still escape from CC subsequently because short-time clamping was not enough for cell adhesion. In the study, we explored another way to enhance cell retention in CC by injecting cell spheroids. We found that the ASs group showed a better therapeutic effect for ED than the FAs group when they had a same cell dose. Moreover, in each ASs group, neither experimental animal deaths nor PE were found. These results suggested that the use of ASs to retain SCs in CC created a satisfactory ED treatment effect with fewer SCs, avoiding the risk associated with PE. Cell trapping within CC was completely dependent on the large sizes of spheroids which could be controlled by adjusting cell numbers. In addition, the strategy was easily manipulated in practice, safe in components and thus should be more conducive for clinical application.

The underlying mechanisms of enhanced ED therapy by stem cell spheroids compared with single cells should be multifold, such as increased cell retention and survival in CC, activated paracrine effect, cell to cell contact, and so on. The increased cell retention by forming spheroids was apparent as demonstrated in the study. From previous reports, forming spheroids would also enhance the anti-apoptotic capacities of mesenchymal stem cells as well as their paracrine effects [34–36]. It was because that the inside of spheroids was somewhat a hypoxic microenvironment. Actually, pre-condition with hypoxia has been used by researchers to enhance MSC survival after transplantation [37]. The hypoxic microenvironment within spheroids may play a similar role like hypoxia-precondition and thus activate the anti-apoptotic capacity and paracrine effect of mesenchymal stem cells. Meanwhile, it

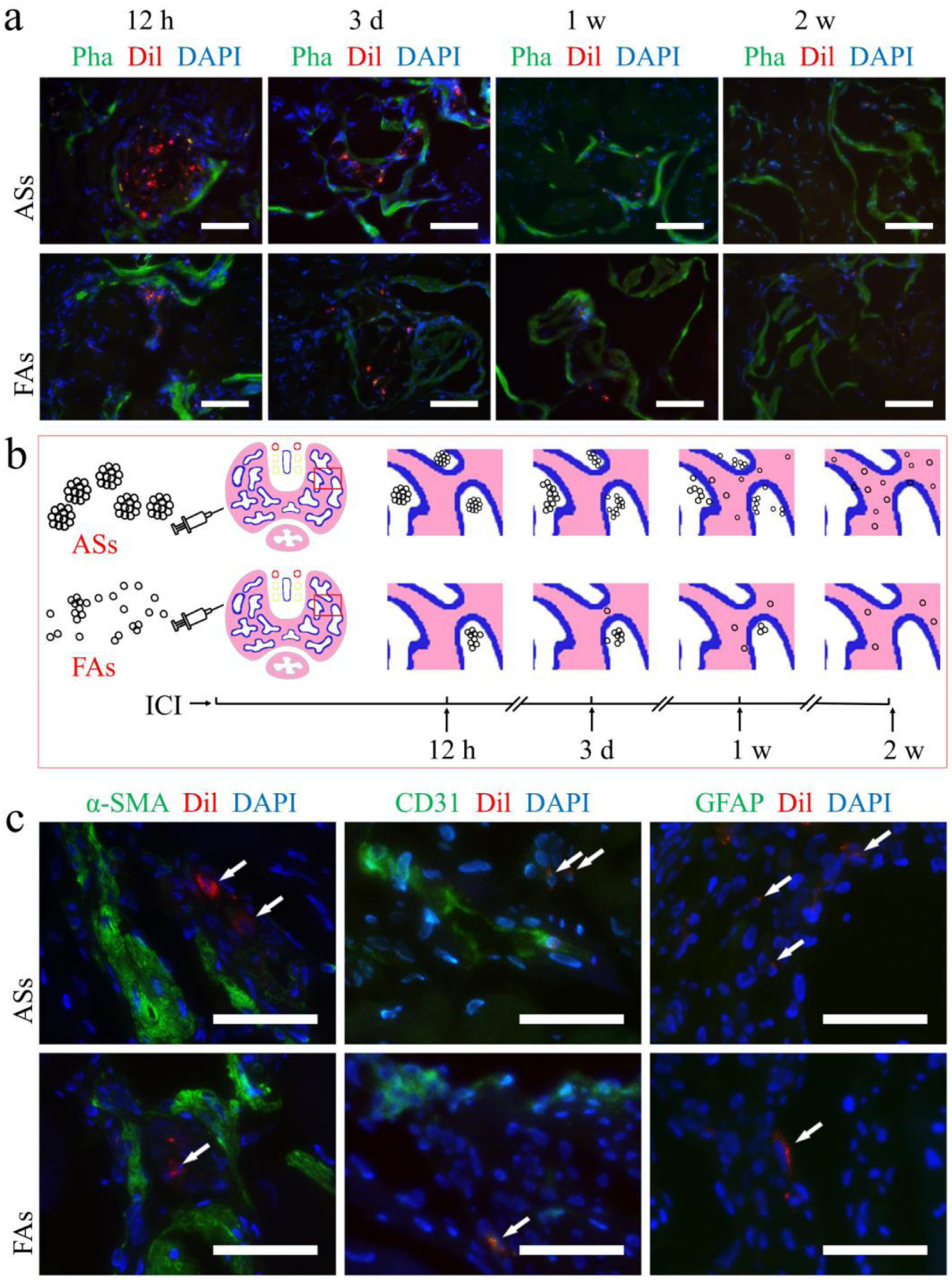

Fig. 6. Dynamic changes and differentiation of ADSCs after injection into the CC. (a) Dynamic changes of trapped ASs and FAs in CC after injection. Green, red, and blue indicating the smooth muscle, Dil-labeled ADSCs and cell nuclei respectively. Scale bar = 100 μm. (b) Schematic view of the dynamic morphological changes of the ASs and cell clusters in the CC. (c) Two weeks after ICI, no differentiation of ADSCs was detected via immunofluorescence. Scale bar = 50 μm. (For interpretation of the references to color in this figure legend, the reader is referred to the web version of this article.)

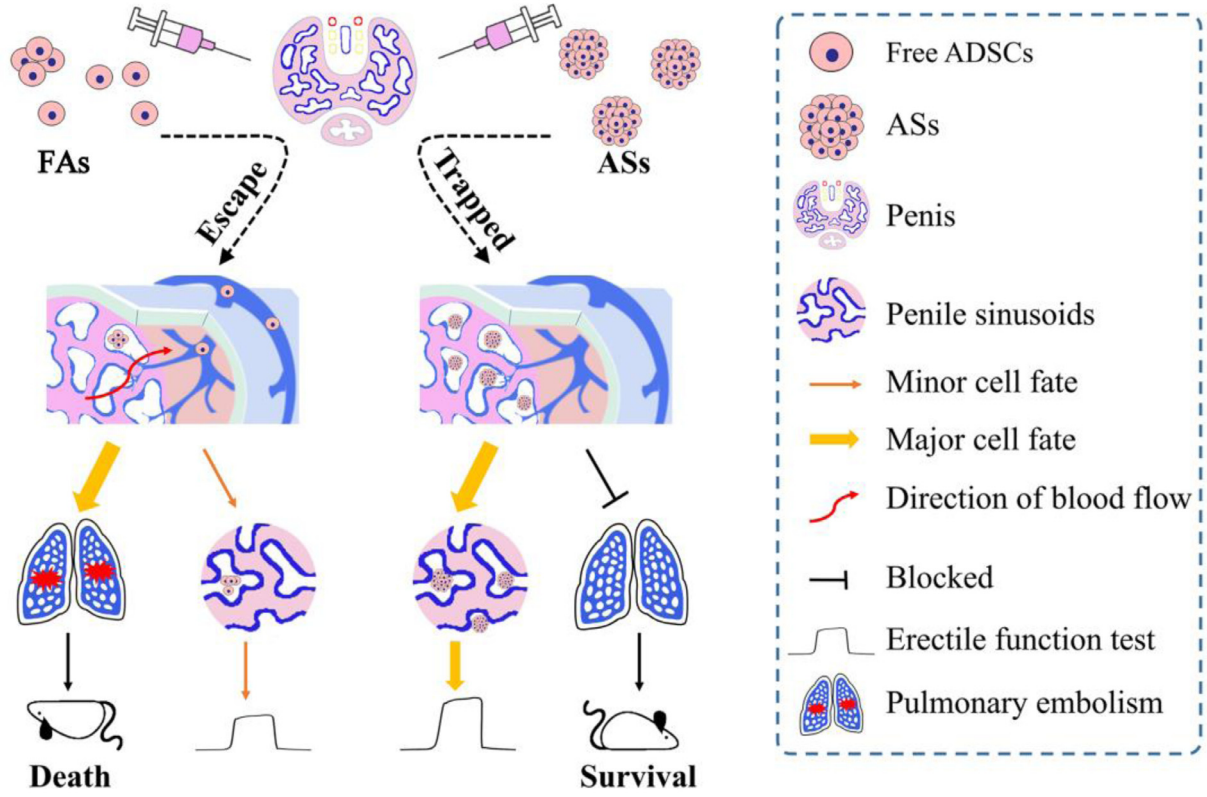

Fig. 7. Schematic illustrating the efficacy and safety of FAs and size-specific ASs for ED therapy through ICI. The cavernous sinusoidal structure made it easy for free cells to escape from CC, leading to reduced therapeutic efficacy for ED and high risk of pulmonary embolism. Conversely, formation of size-specific ASs, whose sizes could be controlled by adjusting cell numbers, is an efficient method to trap stem cells in CC, to improve therapeutic efficacy and to avoid pulmonary embolism.

has been demonstrated that abundant extracellular matrix was secreted within cell spheroids, providing a temporary environment for cell survival after injection and preventing anoikis [35]. Due to the extracellular matrix within spheroids, it would be easier for cells from spheroids to adhere *in vivo*, construct contact with recipient cells and thus promote tissue repair after transplantation [38].

One may concern that necrosis would occur in transplanted spheroids due to the lack of blood supply. However, the study demonstrated that cell spheroids would rapidly spread and grow out *in situ*. Despite, we still think it would be better if vascularized cell spheroids could be prepared and deserved in-depth investigation. Of course, there are also some potential problems that should be paid attention to, e.g., the microenvironments of the SCs in the outer and inner layers of the microsphere are different, whether the difference would result in disparate biological behaviors of ADSCs deserved further investigation too in the future.

In conclusion, we have clarified the formation of scaffold-free spheroids, whose sizes could be controlled by adjusting cell numbers, was an efficient method to trap ADSCs in CC, to improve therapeutic efficacy and to avoid PE. Our results illustrated that ICI of free ADSCs should be cautiously manipulated in practice, while ICI of size-specific spheroids may represent a promising solution and wise choice for future ED therapy.

Declaration of Competing Interest

None of the authors have any relationships/conditions/circumstances that present a potential conflict of interest.

Acknowledgements

This work was supported by the National Natural Science Foundation of China (No. 81701432). Youth Training Project for Medical science (16QNP129) and Beijing Nova Program of science and technology (Z171100001117115). The funders had no role in study design, data collection, data analysis, interpretation, writing of the manuscript.

Supplementary materials

Supplementary material associated with this article can be found in the online version at doi:10.1016/j.ebiom.2020.102656.

References

[1] Geraerts I, Van Poppel H, Devoogdt N, De Groef A, Fieuws S, Van Kampen M. Pelvic floor muscle training for erectile dysfunction and climacturia 1 year after nerve sparing radical prostatectomy: a randomized controlled trial. Int J Impot Res 2016;28(1):9–13.
[2] Walz J, Epstein JI, Ganzer R, Graefen M, Guazzoni G, Kaouk J, et al. A critical analysis of the current knowledge of surgical anatomy of the prostate related to optimisation of cancer control and preservation of continence and erection in candidates for radical prostatectomy: an update. Eur Urol 2016;70(2):301–11.
[3] Sridhar AN, Cathcart PJ, Yap T, Hines J, Nathan S, Briggs TP, et al. Recovery of baseline erectile function in men following radical prostatectomy for high-risk prostate cancer: a prospective analysis using validated measures. J Sex Med 2016;13(3):435–43.
[4] Kendirci M, Bivalacqua TJ, Hellstrom WJ. Vardenafil: a novel type 5 phosphodiesterase inhibitor for the treatment of erectile dysfunction. Expert Opin Pharmacother 2004;5(4):923–32.
[5] McCullough AR, Barada JH, Fawzy A, Guay AT, Hatzichristou D. Achieving treatment optimization with sildenafil citrate (Viagra) in patients with erectile dysfunction. Urology 2002;60(2 Suppl 2):28–38.
[6] Yiou R, Hamidou L, Birebent B, Bitari D, Le Corvoisier P, Contremoulins I, et al. Intracavernous injections of bone marrow mononucleated cells for postradical prostatectomy erectile dysfunction: final results of the instin clinical trial. Eur Urol Focus 2017;3(6):643–5.
[7] Haahr MK, Jensen CH, Toyserkani NM, Andersen DC, Damkier P, Sorensen JA, et al. Safety and potential effect of a single intracavernous injection of autologous adipose-derived regenerative cells in patients with erectile dysfunction following radical prostatectomy: an open-label phase i clinical trial. EBioMedicine 2016;5:204–10.

[8] Bochinski D, Lin GT, Nunes L, Carrion R, Rahman N, Lin CS, et al. The effect of neural embryonic stem cell therapy in a rat model of cavernosal nerve injury. BJU Int 2004;94(6):904–9.
[9] Lin CS, Lin G, Lue TF. Allogeneic and xenogeneic transplantation of adipose-derived stem cells in immunocompetent recipients without immunosuppressants. Stem Cells Dev 2012;21(15):2770–8.
[10] Lin CS, Xin Z, Dai J, Huang YC, Lue TF. Stem-cell therapy for erectile dysfunction. Expert Opin Biol Ther 2013;13(11):1585–97.
[11] Bahk JY, Jung JH, Han H, Min SK, Lee YS. Treatment of diabetic impotence with umbilical cord blood stem cell intracavernosal transplant: preliminary report of 7 cases. Exp Clin Transplant 2010;8(2):150–60.
[12] Gao J, Dennis JE, Muzic RF, Lundberg M, Caplan AI. The dynamic in vivo distribution of bone marrow-derived mesenchymal stem cells after infusion. Cells Tissues Organs 2001;169(1):12–20.
[13] Schrepfer S, Deuse T, Reichenspurner H, Fischbein MP, Robbins RC, Pelletier MP. Stem cell transplantation: the lung barrier. Transplant Proc 2007;39(2):573–6.
[14] Lee RH, Pulin AA, Seo MJ, Kota DJ, Ylostalo J, Larson BL, et al. Intravenous hMSCs improve myocardial infarction in mice because cells embolized in lung are activated to secrete the anti-inflammatory protein TSG-6. Cell Stem Cell 2009;5(1):54–63.
[15] Jung JW, Kwon M, Choi JC, Shin JW, Park IW, Choi BW, et al. Familial occurrence of pulmonary embolism after intravenous, adipose tissue-derived stem cell therapy. Yonsei Med J 2013;54(5):1293–6.
[16] Cyranoski D. Korean deaths spark inquiry. Nature 2010;468(7323):485.
[17] Xu Y, Guan R, Lei H, Li H, Wang L, Gao Z, et al. Therapeutic potential of adipose-derived stem cells-based micro-tissues in a rat model of postprostatectomy erectile dysfunction. J Sex Med 2014;11(10):2439–48.
[18] Xu Y, Xin H, Wu Y, Guan R, Lei H, Fu X, et al. Effect of icariin in combination with daily sildenafil on penile atrophy and erectile dysfunction in a rat model of bilateral cavernous nerves injury. Andrology 2017;5(3):598–605.
[19] Bartosh TJ, Ylostalo JH, Mohammadipoor A, Bazhanov N, Coble K, Claypool K, et al. Aggregation of human mesenchymal stromal cells (MSCs) into 3D spheroids enhances their antiinflammatory properties. Proc Natl Acad Sci USA 2010;107 (31):13724–9.
[20] Gu X, Shi H, Matz E, Zhong L, Long T, Clouse C, et al. Long-term therapeutic effect of cell therapy on improvement in erectile function in a rat model with pelvic neurovascular injury. BJU Int 2019;124(1):145–54.
[21] Kadihasanoglu M, Ozbek E. Intravenous preload of mesenchymal stem cells rescues erectile function in a rat model of cavernous nerve injury. BJU Int 2017;14 (9):1175.
[22] Ficarra V, Novara G, Ahlering TE, Costello A, Eastham JA, Graefen M, et al. Systematic review and meta-analysis of studies reporting potency rates after robot-assisted radical prostatectomy. Eur Urol 2012;62(3):418–30.
[23] Salonia A, Burnett AL, Graefen M, Hatzimouratidis K, Montorsi F, Mulhall JP, et al. Prevention and management of postprostatectomy sexual dysfunctions. part 1: choosing the right patient at the right time for the right surgery. Eur Urol 2012;62(2):261–72.
[24] Salonia A, Adaikan G, Buvat J, Carrier S, El-Meliegy A, Hatzimouratidis K, et al. Sexual rehabilitation after treatment for prostate cancer-part 2: recommendations from the fourth international consultation for sexual medicine (ICSM 2015). J Sex Med 2017;14(3):297–315.
[25] Weyne E, Castiglione F, Van der Aa F, Bivalacqua TJ, Albersen M. Landmarks in erectile function recovery after radical prostatectomy. Nat Rev Urol 2015;12 (5):289–97.
[26] Levy JA, Marchand M, Iorio L, Cassini W, Zahalsky MP. Determining the feasibility of managing erectile dysfunction in humans with placental-derived stem cells. J Am Osteopath Assoc 2016;116(1):e1–5.
[27] Protogerou V, Michalopoulos E. Administration of adipose derived mesenchymal stem cells and platelet lysate in erectile dysfunction: a single center pilot study. Bioengineering (Basel) 2019;6(1):21.
[28] Wu H, Tang WH, Zhao LM, Liu DF, Yang YZ, Zhang HT, et al. Nanotechnology-assisted adipose-derived stem cell (ADSC) therapy for erectile dysfunction of cavernous nerve injury: in vivo cell tracking, optimized injection dosage, and functional evaluation. Asian J Androl 2018;20(5):442–7.
[29] Lin H, Dhanani N, Tseng H, Souza GR, Wang G, Cao Y, et al. Nanoparticle improved stem cell therapy for erectile dysfunction in a rat model of cavernous nerve injury. J Urol 2016;195(3):788–95.
[30] Wei DX, Dao JW, Chen GQ. A micro-ark for cells: highly open porous polyhydroxyalkanoate microspheres as injectable scaffolds for tissue regeneration. Adv Mater 2018;30(31):e1802273.
[31] Sondermeijer HP, Witkowski P, Seki T, van der Laarse A, Itescu S, Hardy MA. RGDfK-Peptide modified alginate scaffold for cell transplantation and cardiac neovascularization. Tissue Eng Part A 2018;24(9–10):740–51.
[32] You D, Jang MJ, Kim BH, Song G, Lee C, Suh N, et al. Comparative study of autologous stromal vascular fraction and adipose-derived stem cells for erectile function recovery in a rat model of cavernous nerve injury. Stem Cells Transl Med 2015;4(4):351–8.
[33] Liu Y, Zhao S, Luo L, Wang J, Zhu Z, Xiang Q, et al. Mesenchymal stem cell-derived exosomes ameliorate erection by reducing oxidative stress damage of corpus cavernosum in a rat model of artery injury. J Cell Mol Med 2019;23(11):7462–73.
[34] Zhao X, Qiu X, Zhang Y, Zhang S, Gu X, Guo H. Three-Dimensional aggregates enhance the therapeutic effects of adipose mesenchymal stem cells for ischemia-reperfusion induced kidney injury in rats. Stem Cells Int 2016;2016:20169062638.
[35] Bhang SH, Cho SW, La WG, Lee TJ, Yang HS, Sun AY, et al. Angiogenesis in ischemic tissue produced by spheroid grafting of human adipose-derived stromal cells. Biomaterials 2011;32(11):2734–47.
[36] Bartosh TJ, Ylostalo JH, Mohammadipoor A, Bazhanov N, Coble K, Claypool K, et al. Aggregation of human mesenchymal stromal cells (MSCs) into 3D spheroids enhances their antiinflammatory properties. Proc Natl Acad Sci USA 2010;107 (31):13724–9.
[37] Shin HS, Lee S, Kim YM, Lim JY. Hypoxia-Activated adipose mesenchymal stem cells prevents irradiation-induced salivary hypofunction by enhanced paracrine effect through fibroblast growth factor 10. Stem Cells 2018;36(7):1020–32.
[38] Potapova IA, Brink PR, Cohen IS, Doronin SV. Culturing of human mesenchymal stem cells as three-dimensional aggregates induces functional expression of CXCR4 that regulates adhesion to endothelial cells. J Biol Chem 2008;283 (19):13100–7.